The first real-time worldwide ionospheric predictions network: an advance in support of spaceborne experimentation, on-line model validation, and space weather

GEOPHYSICAL RESEARCH LETTERS, VOL. 25, NO. 4, PAGES 449-452, FEBRUARY 15, 1998

The first real-time worldwide ionospheric predictions network: An advance in support of spaceborne experimentation, on-line model validation, and space weather

E.P. Szuszczewicz[1], P. Blanchard[1], P. Wilkinson[2], G. Crowley[3], T. Fuller-Rowell[4], P. Richards[5], M. Abdu[6], T. Bullett[7], R. Hanbaba[8], J. P. Lebreton[9], M. Lester[10], M. Lockwood[11], G. Millward[4], M. Wild[10], S. Pulinets[12], B.M. Reddy[13], I. Stanislawska[14], G. Vannaroni[15], and B. Zolesi[16]

Abstract. We report on the first realtime ionospheric predictions network and its capabilities to ingest a global database and forecast F-layer characteristics and "in situ" electron densities along the track of an orbiting spacecraft. A global network of ionosonde stations reported around-the-clock observations of F-region heights and densities, and an on-line library of models provided forecasting capabilities. Each model was tested against the incoming data; relative accuracies were intercompared to determine the best overall fit to the prevailing conditions; and the best-fit model was used to predict ionospheric conditions on an orbit-to-orbit basis for the 12-hour period following a twice-daily model test and validation procedure. It was found that the best-fit model often provided averaged (i.e., climatologically-based) accuracies better than 5% in predicting the heights and critical frequencies of the F-region peaks in the latitudinal domain of the TSS-1R flight path. There was a sharp contrast, however, in model-measurement comparisons involving predictions of actual, unaveraged, along-track densities at the 295 km orbital altitude of TSS-1R. In this case, extrema in the first-principle models varied by as much as an order of magnitude in density predictions, and the best-fit models were found to disagree with the "in situ" observations of N_e by as much as 140%. The discrepancies are interpreted as a manifestation of difficulties in accurately and self-consistently modeling the external controls of solar and magnetospheric inputs and the spatial and temporal variabilities in electric fields, thermospheric winds, plasmaspheric fluxes, and chemistry.

1. Introduction

Intelligent operations of many of today's near-Earth space experiments and the effective utilization of space-based technology assets are looking more and more to accurate and timely forecasting of the Earth's space environment. Such a capability is seen to be critical to enhancing scientific productivity during interactive on-orbit experimentation as well as to the mitigation of, or protection from, space environmental effects on man-made systems.

Realtime monitoring and prediction are also becoming increasingly important for effective and efficient execution of large system science programs like those in NASA's International Solar-Terrestrial Physics program (e.g. Berchem et al., 1995) and the National Space Weather Initiative (e.g., Szuszczewicz, 1995). These programs involve large databases with inputs from an array of ground-based and spaceborne sensors, and more often than not, employ a suite of large computational codes used in the planning, execution, and analysis of campaign investigations.

The SUNDIAL/TSS-1R activity reported here (see, e.g., Szuszczewicz et al., 1996, Dobrowolny and Stone, 1994; and Stone and Bonifazi, 1997 (this issue)) was the first demonstrated world-wide effort to meet this need. The effort focused on supporting TSS-1R objectives which dealt with the conduct and analysis of experiments exploring plasma processes and related technologies that control current generation and current closure in space, on-orbit power generation techniques, and associated manifestations in current-voltage characteristics and spacecraft charging. In meeting these objectives the primary geophysical parameter was the ionospheric electron density acting through its first-order control of conductivities and plasma sheaths.

While functional objectives and an on-orbit time-line are established well in advance of any mission, an optimized experiment scenario dictates realtime or near-realtime access and analysis of on-board data (e.g., spacecraft potentials, current-voltage characteristics, etc.), with subsequent interpretations possibly leading to the need for a repeat of certain functional objectives under identical, different, or more ideal conditions. This generated the need for a realtime worldwide ionospheric monitoring network and a capability to predict along-track plasma densities on time scales ranging from orbit-to-orbit to a full 24 hr period. We describe the network, the data ingestion procedures, prediction methodologies, and initial results on prediction accuracies.

2. Orbit Logistics, the Worldwide Monitoring Network, and the Prediction Methodology

TSS-1R was launched on February 22, 1996 (UT day/hr:min = 53/20:18) into a 28.5° inclination orbit at an altitude of 295 km. With the height of the F_2-region peak-density generally varying between 200 and 600 km, TSS-1R experiments were expected to operate in plasma density environments generally less that $4(10)^6$ cm^{-3} but greater than $(10)^4$ cm^{-3}, with the orbiter and the tethered subsatellite operating variously at, above, or below the F_2-region peak.

Since the worldwide monitoring of plasma densities at 295 km is technically not feasible (this statement is true for any fixed altitude), the monitoring and predictions approach employed in this application was built upon a combination of internationally-

[1]Science Applications International Corporation, McLean, Virginia
[2]IPS Radio & Space Services, West Chatswood, Australia
[3]Southwest Research Institute, San Antonio, Texas
[4]National Oceanic and Atmospheric Administration, Boulder, Colorado
[5]University of Alabama, Huntsville, Alabama
[6]Instituto Nacional de Pesquisas Espaciais, Sao Paulo, Brazil
[7]Phillips Lab, Hanscom AFB, Massachusetts
[8]France Telecom/CNET, Lannion, France
[9]Space Science Department, ESA/ESTEC, Nordwijk, The Netherlands
[10]University of Leicester, Leicester, United Kingdom
[11]Rutherford Appleton Lab, Oxon, United Kingdom
[12]IZMIRAN, Moscow Region, Russia
[13]National Geophysical Research Institute, Hyderabad, India
[14]Space Research Center, Warsaw, Poland
[15]Instituto di Fisica Dello Spazio Interplanetario, Frascati, Italy
[16]Instituto Nazionale di Geofisica, Italy

Paper number 97GL03279.
0094-8534/98/97GL-03279$05.00

recognized models and a globally-distributed network of ionosondes for around-the-clock measurements of F-region characteristics. The ionosonde database provided a nowcasting capability and the framework for benchmarking model accuracies, establishing optimal fits to prevailing conditions, and subsequent forecasting by the model run best matching the realtime data. The accuracy of the optimized model fit to the global ionosonde measurements of N_mF_2 and h_mF_2 was assumed to provide a measure of confidence that model values of electron densities at the TSS-1R altitude were of comparable accuracy.

There were 33 ionosonde stations employed in support of TSS-1R, a subset of the 50-70 stations typically engaged in worldwide SUNDIAL campaigns (e.g., Szuszczewicz et al., 1996; and references therein). The reduced number reflected a conservative approach to the operation of a first realtime data ingestion procedure and an on-the-fly requirement for model optimization. The procedure was as follows:

1) Every 12 hours each of the 33 stations transmitted an up-to-the-hour set of data via Internet to the SUNDIAL Ionospheric Weather Station in the TSS-1R Science Operations Center. The data provided hourly values of f_oF_2 and M(3000)F_2 for that 12-hour period. M(3000)F_2 yielded values of h_mF_2 in accordance with the procedures of Dudeney [1983] and the critical frequency of the F_2-peak, f_oF_2, provided a measurement of N_mF_2 through the relationship f_oF_2 (Hz) = $8.9(10^3)\sqrt{N_mF_2\ [cm^{-3}]}$. (Most of the 33 stations could transmit data on a more frequent basis, e.g. hourly (or fractions thereof) if dictated by future mission requirements.)

2) The database was then compared with an on-line library of model runs that included: a) the International Reference Ionosphere, IRI (Schunk and Szuszczewicz, 1988, and references therein), b) the Field-Line Interhemispheric Plasma model, FLIP (Richards et al., 1994; and references therein), c) the Coupled Thermospheric Ionospheric Plasmasphere model, CTIP (Fuller-Rowell et al. 1996; and references therein), and d) the Thermosphere Ionosphere Electrodynamics General Circulation Model, TIEGCM (Richmond et al., 1992; and references therein). Multiple on-line runs of FLIP and TIEGCM, expected to bracket ranges of solar fluxes and geomagnetic conditions predicted by the NOAA Space Environment Center (70 ≤ 10.7 cm flux ≤ 76, 5 ≤ Ap ≤ 10, and kp ≤ 3), were compared against the data. A single "best-guess" run of the CTIP model and several cases of the IRI (with varying values for the sunspot number and several sliding 30 day averages bracketed by 1 February and 31 March) were also compared against the data. (The first-principle model runs were completed several weeks before the mission and installed in the on-line library for on-the-fly comparisons with the data. We note that no model is rigorously "first-principle", since all rely, to varying degrees, on empirically-based boundary conditions or force descriptions. This is true of all models in the specification of solar and magnetospheric inputs; and as an example of empirically-based inputs for internal driving forces, the FLIP model uses IRI specifications of h_mF_2 to effectively allow for influences of thermospheric winds at mid-latitudes and electric fields at low-to-equatorial latitudes.)

3) The runs of each model which best fit the data were then intercompared, and the "best-of-the-best" was selected to predict the orbit-to-orbit along-track densities for the next 12 hours.

4) New data were ingested every 12 hours and the procedure repeated, with the orbit-to-orbit predictions posted on an "Ionospheric Weather Board" in the Science Operations Center.

In varying degrees the models represented the coupled ionospheric-thermospheric system - each with different approaches to the prevailing physics and different levels of computational complexity. The IRI is a PC-based empirical model. FLIP, CTIP, and TIEGCM are first-principle models. FLIP, CTIP and TIEGCM are VAX-, workstation, and Cray-based, respectively.

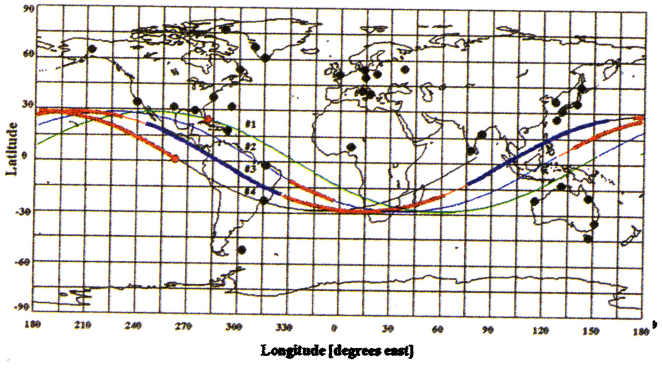

Plate 1. Ground tracks for four TSS-1R orbits covering the period from the initial fly-away (red dot, orbit #1) through the tether break (red dot, orbit #4). Black dots identify ionosonde stations.

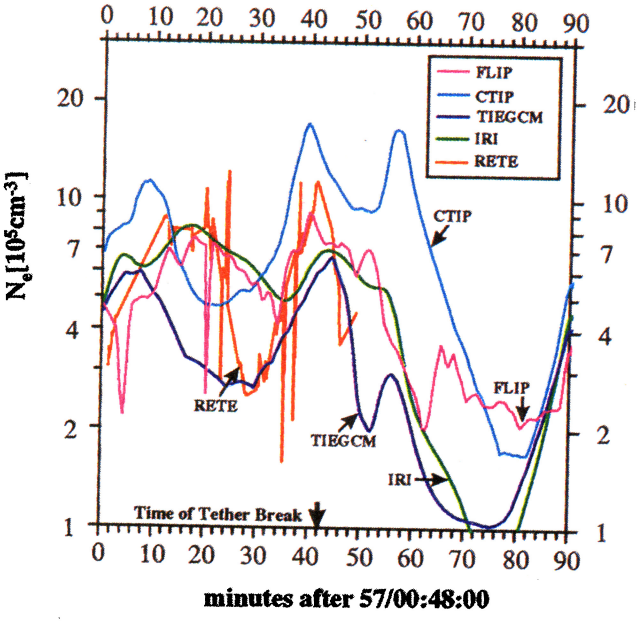

Plate 2. Along-track density predictions compared with "in situ" data from the RETE Langmuir probe.

3. Results

We concentrate on the segment of the TSS-1R mission from the initial subsatellite deployment (UT = 56/20:45, defined as the "fly-away") to the tether break (UT = 57/01:29). This involved the four orbits shown in Plate 1, defined here as orbits 1 through 4, color-coded by the thin green, blue, red, and black lines, respectively. The black dots identify the ionosonde stations, while the two red dots identify the locations of the initial fly-away (on green orbit #1) and the location of the orbiter at the time of the tether break (on black orbit #4). The bold red and blue overlays on the orbit tracks identify functional objective periods IV and DC (Stone and Bonifazi, 1997 (this issue)), respectively, in which tether current-voltage characteristics were studied. While there were orbit-to-orbit differences, the general diurnal characteristics of the ionospheric conditions encountered by the orbiter during orbits 1-4 were such that sunrise and sunset were approximately at 90° E and 270° E longitudes, respectively. The descending node in the late afternoon and early evening period (i.e., 210° ≤ long ≤ 270°) therefore crossed the region of the Appleton Anomaly (see e.g., Klobuchar et al., 1991 and references therein. This was the ionospheric domain encountered just after fly-away and just after the tether break.

The SUNDIAL ionospheric weather activities supporting the four-orbits involved data ingestion, model fit, and prediction updates at UT = 56/16:00, 57/04:00, and 57/16:00. We summarize the accuracies of each best-fit-model-run in Table 1 (% accuracy = 100 x (model-data)/data). The results show accuracies of the best-fits to f_oF_2 and h_mF_2 cataloged according to day/night (D/N) time frames.

Table 1. Model Accuracies (%) at Low Latitudes ($\leq 30°$)

Observable —>		f_oF_2			h_mF_2		
Time of Data Ingest —>		56/16:00	57/04:00	57/16:00	56/16:00	57/04:00	57/16:00
IRI	D	$0.4^{8.3}_{-4.6}$	$1.3^{5.5}_{-4.6}$	$-0.7^{3.4}_{-6.7}$	$5.0^{12.5}_{-2.8}$	$5.2^{14.0}_{-6.3}$	$5.3^{12.1}_{-10.4}$
	N	$5.6^{14.6}_{-4.5}$	$3.6^{15.9}_{-8.9}$	$-3.6^{5.7}_{-11.1}$	$-0.9^{7.3}_{-4.9}$	$-3.6^{6.8}_{-10.8}$	$-5.4^{5.1}_{-13.2}$
TIEGCM	D	$-5.3^{21.0}_{-12.1}$	$-4.6^{7.0}_{-12.8}$	$-7.1^{7.0}_{-15.0}$	$6.3^{14.5}_{0.1}$	$6.6^{15.2}_{-1.2}$	$7.0^{14.3}_{-5.9}$
	N	$3.4^{21.6}_{-10.9}$	$1.1^{14.1}_{-8.2}$	$-5.2^{6.1}_{-10.4}$	$5.3^{11.0}_{2.3}$	$2.3^{11.4}_{-1.3}$	$0.5^{9.4}_{-5.9}$
FLIP	D	$3.7^{15.7}_{-0.8}$	$5.1^{11.6}_{0.0}$	$1.9^{6.5}_{-2.5}$	$5.0^{11.5}_{-2.3}$	$5.3^{12.9}_{-5.5}$	$5.7^{11.7}_{-10.0}$
	N	$18.4^{27.6}_{4.8}$	$14.6^{23.4}_{4.6}$	$5.5^{14.8}_{-0.9}$	$0.3^{8.2}_{-4.3}$	$-1.5^{8.7}_{-10.4}$	$-3.4^{6.9}_{-12.7}$
CTIP	D	$25.6^{43.5}_{17.1}$	$26.7^{35.7}_{16.4}$	$22.4^{28.7}_{13.9}$	$6.0^{11.9}_{1.0}$	$6.5^{13.3}_{1.1}$	$6.3^{11.8}_{-3.3}$
	N	$53.5^{-73.0}_{26.9}$	$49.4^{76.5}_{25.4}$	$36.7^{66.4}_{8.5}$	$-0.6^{7.1}_{-6.4}$	$-2.5^{7.9}_{-9.2}$	$-4.6^{5.4}_{-8.5}$

The largest-font numerical entry represents the accuracy of the model fit averaged over the full daytime (or nighttime) period, while the smaller-font numerical entries (super- and subscripted) represent the extrema of the hourly accuracies during that same period. (We note that the same best-fit run of each model prevailed from data-report-period to data-report-period. As a consequence, the 2nd and 3rd reporting periods tested the accuracy of the model predictions developed during the previous 12-hr data-ingest and model-fit period.)

Table 1 shows that during daytime periods the IRI consistently provided the best accuracies in both f_oF_2 and h_mF_2; while at night, best-fit honors in f_oF_2 were generally shared by the IRI and the TIEGCM, with differences generally not in excess of 2 percent. In terms of nighttime values for h_mF_2, all model accuracies tended to be comparable, with the IRI and FLIP models the leaders. (We note that slight differences in their respective h_mF_2 accuracies [remembering that FLIP uses IRI specifications for h_mF_2] are a result of differences in selecting the sunspot numbers that initiated the IRI.) In the realtime operations, the IRI was the model selected as "best-of-the-best" as a result of its overall day/night and f_oF_2/h_mF_2 accuracies.

Discussed thus far have only been the accuracies relative to N_mF_2 and h_mF_2 as measured by the ionosondes. The ultimate TSS-1R test involved the along-track N_e accuracy at the orbiter and/or the tethered subsatellite. Plate 2 provides a measure of this accuracy for the subsatellite during orbit 4 (which involved the tether break), with each of the best-fit along-track model predictions compared against an "in situ" density measurement by a Langmuir probe that was part of the RETE (Research on Electrodynamic Tether Effects) instrument complement (Dobrowolny et al., 1994). (The discontinuities in the RETE results stem from attempts to correct for known periods involving sheath-effect perturbations and/or to delete data collected during periods of perturbed satellite potentials [G. Vannaroni and J.-P. Lebreton, private communication]).

With reference to Plate 2 we offer the following observations: 1) all models show the qualitative feature of the Appleton Anomaly (i.e., the double peaks in the time frame between 30 and 65 minutes after 57/00:48) but all differ in the intensity and location of the peaks; and 2) qualitatively and quantitatively the along-track RETE data agree best with the IRI and FLIP results between 10 and 25 minutes (after 57/00:48) and again between 33 and 40 minutes (after 57/00:48), while there is better agreement between RETE data and the TIEGCM results in the period between 25 and 32 minutes (after 57/00:48). This latter period encompasses the late afternoon ionospheric domain with cooling temperatures and descending values for h_mF_2.

Plate 2 also reveals a broad range of model predictions, (with, for example, CTIP and TIEGCM differing by nearly an order of magnitude) a result that might be considered unexpected given the prevaling low-solar and low-to-moderate geomagnetic activities. However, at low latitudes ionospheric densities are particularly sensitive to electric fields (yet to be accurately modeled) with variability driven by the E and F region dynamo winds. (There may also be magnetospherically-imposed fields during storms, but such was not the case in this period.) Other issues involve the controls of the topside and bottomside gradients, which tend to dominate the domain of N_e sampling in Plate 2, a topic discussed in the following section. (In the version of CTIP used here, an equatorial zonal electric field for moderately-high solar activity was employed. This turned out to be unrealistically high for the prevailing conditions, and accounts for some of the large differences in the models. We also note that recent work on TIEGCM by Crowley and Fesen (pvt. comm., 1997) appears to provide significant improvements in low-latitude dynamo effects.)

4. Comments and Conclusions

Based on daytime and nighttime averages (Table 1), the optimized model fits to the database and subsequent predictions of F_2-region heights and densities were very good, with the "best-of-the-best" yielding averaged f_oF_2 and h_mF_2 accuracies generally better than 5%. (We note, however, that typical non-averaged hourly extrema of the "best-of-the-best" model extended to values near 15%.) Much of this goodness-of-fit is due to the fact that overall conditions were predominantly quiet-to-moderately disturbed (i.e., $0 \leq kp \leq 3$ for the majority of the reporting periods) - conditions under which models are expected to perform optimally. Other factors contributing to the overall goodness-of-fit deal with the averaging process itself, which provided more of a climatological perspective (again, a framework in which models are expected to perform optimally). The combination of these circumstances provided an environment in which the IRI would be expected to perform especially well. It is an empirically-based model which represents the sum total of all cause-effect relationships as manifested by nature itself. In the case of the first-principle models, the cause-effect terms are at the root of the individual approaches and a number of controlling forces upon which the models are based are still under investigation (see e.g., Szuszczewicz, 1995; and Szuszczewicz et al., 1996).

In comparing the along-track N_e measurements with model predictions (Plate 2), we find the results in sharp contrast with the Table 1 comparisons discussed in the previous paragraph. The difference is traceable to several issues, including relative abilities to model climatologies (i.e., averaged behaviors) versus abilities to model weather (i.e., day-to-day and hour-to-hour variability). Other issues involve, on the one hand, the comparison of densities at the

F-peak (i.e., Table 1), where a great deal of data have been available for model development studies. On the other hand, there is the comparison with densities at a fixed altitude (i.e., Plate 2) which cuts across the F-peak and involves bottomside and topside gradients where little data have been available and few model development studies have been carried out. The results are rather sobering, when one notes almost an order of magnitude difference between CTIP and TIEGCM predictions, and differences as large as 140 % between the IRI and RETE values for N_e (see, e.g., Fig. 2 near 28 minutes after 48:00). This reflects the difficulty of properly and self-consistently modeling the controlling forces, with those on the topside being primarily electric fields, diffusion, and plasmaspheric fluxes, while those on the bottomside are electric fields, winds, and chemistry. These forces are fundamental to all ionospheric-physics, but electric fields are especially critical at low-to-equatorial latitudes. It is the electric fields that are the primary agent for the development of the Appleton Anomaly, with winds playing a secondary role. Within this context we note that overall agreement is best among the data and the FLIP and IRI predictions, because those models effectively include the prevailing electric fields through their empirical specification of h_mF_2. (We note that the fine structure and occasional discontinuities in the FLIP results in Plate 2 are related to the fact that the model solution is carried out along separate flux tubes, each with its own unique set of conditions, and the fact that the plot requires interpolation onto the continuous orbital track between locations of flux tube solutions.)

In general, it is understood that day-to-day and hour-to-hour variability is traceable to variations in atmospheric gravity waves, tidal controls, high latitude inputs, and solar EUV fluxes. These drive the winds, thermospheric densities, temperatures, and electric fields - all of which control chemistry, diffusion, and transport - and ultimately the electron density. A recent study [Szuszczewicz et al. 1996] has shown that the modeling of these forces is not well in hand, with specific issues addressing the accuracy in climatological perspectives of thermospheric winds, plasmaspheric fluxes and electric fields. Clearly, more work is necessary on the fundamental controls of the ionosphere and on data-model comparisons in order to better understand the physics and develop a more accurate space weather predictive capability.

Plans for follow-up activities include detailed views on regional and local station results, with emphasis on model accuracies within large-scale phenomenological domains (e.g., the Appleton Anomaly, the sunrise/sunset terminator, etc.). Attention will also be directed at model-specific assumptions and the density gradients above and below the F_2 peak, since these greatly influence the degree to which models and data agree.

Acknowledgment. The SAIC activity was supported by NASA under contract NAS8-36811. Thanks are extended to the institutions throughout the world which support ionosonde operations. Thanks are also extended to NSF for supporting the modeling efforts of G. Crowley under grant ATM-9696234.

References

Berchem, J., J. Raeder, R.J. Walker, and M. Ashour-Abdalla, Interactive visualization of numerical simulation results: A tool for mission planning and data analysis in *Visualization Techniques in Space and Atmospheric Sciences*, E.P. Szuszczewicz and J. Bredekamp, Eds., NASA SP-519, National Aeronautics and Space Administration, Washington, D.C. (1995)

Dobrowolny, M., E. Melchioni, U. Guidoni, L. Icss, M. Maggi, R. Orfei, Y. de Conchy, C.C. Harvey, R.M. Manning, F. Wouters, J.-P. Lebreton, S. Ekholm, and A. Butler, The RETE experiment for the TSS-1 mission, *Nuovo Cimento, 17*, 101-121, 1994.

Dobrowolny, M. and N.H. Stone, A technical overview of TSS-1: the first tethered-satellite system mission, *Nuovo Cimento, 17*, 1-12, 1994.

Dudeney, J.R., The accuracy of simple methods for determining the height of the maximum electron concentration of the F2-layer from scaled ionospheric characteristics, *J. Atmos. Terr. Phys., 45*, 629, 1983.

Fuller-Rowell, T.J., M.V. Codrescu, R.J. Moffett, and S. Quegan, Response of the thermosphere and ionosphere to geomagnetic storms, *J. Geophys. Res., 99*, 3893-3914, 1994.

Kamide, Y., R.L. McPherron, W.D. Gonzalez, D.C. Hamilton, H.S. Hudson, J.A. Joselyn, S.W. Kohler, L.K. Lyons, H. Lundstedt, and E. Szuszczewicz, Magnetic Storms, *in Proceedings of the Chapman Conference on Magnetic Storms*, B.T. Tsurutani, W.D. Gonzalez, Y. Kamide and J.K. Arballo, eds., JPL Pasadena, CA, AGU Monograph (1997, in press).

Klobuchar, J.A., D.N. Anderson, and P.H. Doherty, Model studies of the latitudinal extent of the equatorial anomaly during equinoctial conditions, *Rad. Science, 26*, 1025-1047, 1991.

Richards, P.G., D.G. Torr, M.J. Buonsanto, and D.P. Sipler, Ionospheric effects of the March 1990 magnetic storm: comparison of theory and measurement, *J. Geophys. Res., 99*, 23,359-23,365, 1994.

Richmond, A.D., Ridley, E.C., and Roble, R.G., A thermosphere/ionosphere general circulation model with coupled electrodynamics, *Geophys. Res. Lett., 19*, 601-604, 1992.

Schunk, R.W., and E.P. Szuszczewicz, First principle and empirical modeling of the global-scale ionosphere, *Ann. Geophys., 6*, 19, 1988.

Stone, N., and C. Bonifazi, The TSS-1R mission: Overview and scientific context, *Geophys. Res. Lett.*, (1997, this issue).

Szuszczewicz, E.P., Advances in ionospheric physics: roles, relevance and predictions in the system of solar-terrestrial plasmas, *U.S. Nat'l Rpt. to IUGG 1991-1994, Reviews of Geophys. Supplement*, 721-728, 1995.

Szuszczewicz, E.P., D. Torr, P. Wilkinson, P. Richards, R. Roble, B. Emery, G. Lu, M. Abdu, D. Evans, R. Hanbaba, K. Igarashi, P. Jiao, M. Lester, S. Pulinets, B.M. Reddy, P. Blanchard, K. Miller, J. Joselyn, F region climatology during the SUNDIAL/ATLAS 1 campaign of March 1992: Model-measurement comparisons and cause-effect relationships, *J. Geophys. Res., 101*, 26,741-26,758, 1996.

M. Abdu, Instituto Nacional de Pesquisas Espaciais, Sao Paulo, Brazil.
P. Blanchard and E.P. Szuszczewicz, Science Applications International Corporaation, 1710 Goodridge Drive, P.O. Box 1303, McLean, VA 22102.
T. Bullett,Phillips Lab, Hanscom AFB, Massachusetts.
G. Crowley,Southwest Research Institute, San Antonio, Texas.
T. Fuller-Rowell, National Oceanic and Atmospheric Administration, Boulder, Colorado.
R. Hanbaba, France Telecom/CNET, Lannion, France
J.P. Lebreton, Space Science Department, ESA/ESTEC, Nordwijk, The Netherlands.
M. Lester and M. Wild, University of Leicester, Leicester, United Kingdom.
M. Lockwood, Rutherford Appleton Lab, Oxon, United Kingdom.
G. Millward, National Oceanic and Atmospheric Administration, Boulder, Colorado.
S. Pulinets, IZMIRAN, Moscow Region, Russia.
B.M. Reddy, National Geophysical Research Institute, Hyderabad, India.
P. Richards, University of Alabama, Huntsville, Alabama.
I. Stanislawska, Space Research Center, Warsaw, Poland.
G. Vannaroni, Instituto di Fisica Dello Spazio Interplanetario, Frascati, Italy.
P. Wilkinson, IPS Radio & Space Services, West Chatswood, Australia.
B. Zolesi, Instituto Nazionale di Geofisica, Italy.

(Received January 15, 1997; revised October 27, 1997;
accepted October 30, 1997)